Producing Chromium Carbide Using Reduction of Chromium Oxide with Methane

B. Khoshandam and R. V. Kumar
Dept. of Materials Science & Metallurgy, University of Cambridge, Cambridge, U.K.

E. Jamshidi
Dept. of Chemical Engineering, Amir-Kabir University (Tehran Polytechnic), Tehran, Iran

DOI 10.1002/aic.10712
Published online October 28, 2005 in Wiley InterScience (www.interscience.wiley.com).

In the present work, reduction of chromium oxide using methane is investigated. The thermogravimetric method was used to obtain kinetic parameters of the reaction in the temperature range of 870-975°C under atmospheric pressure. The experimental data was analyzed using the grain model. The reaction product, chromium carbide, was observed to be produced at a temperature of about 140°C lower than by other conventional methods. Carbon deposition, which is highly undesirable in the synthesis of chromium carbide, was negligible in the present experiments. The experiments were conducted in two modes, either under the conditions of reaction control or under the conditions of diffusion control for determining reaction rate constants and diffusion rates to study pore diffusion, respectively. The pore diffusion studies were carried out with and without considering the bulk flow effect. The gas phase diffusion coefficient through the product layer around the grains was calculated with an approximate method.© 2005 American Institute of Chemical Engineers *AIChE J,* 52: 1094–1102, 2006
Keywords: chromium carbide, chromium oxide, methane, kinetic parameters, grain model

Introduction

The carbides of metallic elements belonging to the transition groups (IV-VI) of the periodic table have properties of high melting points, good strength, low vaporization rate, low vapor pressure at high temperatures, and a good corrosion resistance. Chromium carbide films are used for protecting steel and other alloys from chemical attacks. Indeed, they can be used to produce diamonds and as erosive tools.

There are three forms of chromium carbides (Cr_3C_2, Cr_7C_3, and $Cr_{23}C_6$) with different atomic ratios of carbon to chromium element. Of these carbides, Cr_3C_2 has a good set of properties of high strength, very good coverage resistance, low density, and good chemical stability. This compound has a very high resistance against corrosion and oxidation up to 900°C, and it dissociates only at very high temperature of 1813°C. It is used as an additive in the production of high strength and high wear hardfacing metallic alloys, such as WC-Co, to prevent grain growth. Cr_3C_2 is harder than steel and softer than tungsten carbides.

The chromium carbides are produced using a number of different methods: synthesis from constituent elements, reduction of oxides, deposition from the gaseous phase, electrolysis of molten salts, and chemical precipitation.[1] Reduction of metal oxides with carbon is the most widely used method for producing carbides. Popov et al.[2] showed that producing Cr_3C_2 using reduction of Cr_2O_3 with carbon is carried out at a temperature range of 1100-1270°C. Indeed, based on Berger et al.'s[3] experiments, Cr_3C_2 is produced at a minimum temperature of 1000°C. In the present work, synthesis of Cr_3C_2 is

Correspondence concerning this article should be addressed to R. V. Kumar at rvk10@cam.ac.uk.

Table 1. Results of Thermodynamic Calculations

Products			
(1) Gas Phase			
Component	T = 870°C Mole %	T = 975°C Mole %	T = 1027°C Mole %
H_2	96.417	88.853	73.870
CH_4	2.317	0.876	0.425
CO	1.205	10.120	25.495
H_2O	0.061	0.141	0.175
CO_2	6.595×10^{-4}	0.010	0.035
Total moles	25.714	28.651	34.715
(2) Solid Phase			
Component	T = 870°C Mole	T = 975°C Mole	T = 1027°C Mole
Cr_3C_2	0.072	0.655	1.986
Cr_2O_3	2.891	2.018	0.021
C-graphite	11.949	8.537	0.018

shown to be possible at a temperature as low as 870°C by reducing chromium oxide with methane. Using methane rather than carbon to reduce metal oxides can produce carbides at a lower temperature. For successful use of this method, it is important to avoid the deposition of graphite. The present experiments have shown negligible graphite deposition, thus providing a sound rationale for further development of a process for producing chromium carbide. Therefore, reduction of metal oxides using methane can be a significant method to produce carbides in comparison with other methods.

The chemical reaction between chromium oxide and methane is considered to be as shown below:

$$\frac{3}{13}Cr_2O_3 + CH_4 \rightarrow \frac{2}{13}Cr_3C_2 + \frac{9}{13}CO + 2H_2 \quad (1)$$

The equilibrium constant of the above reaction as a function of temperature is:

$$K_P = \exp\left(27.955 - \frac{30837}{T}\right) \quad (2)$$

The equilibrium constant of the reaction increases from a value of 2.7 at 870°C to 15.5 as the temperature is increased to 950°C, and the reaction becomes very favorable.

Thermodynamic calculations for the minimization of the Gibbs free energy were carried out using the EQUILIB computer program. This program is one of the modules of the FactSage package that is able to perform equilibrium calculations for heterogeneous phase reactions. Further information about this package is presented in the literature.[4] Equilibrium calculations for the reaction between Cr_2O_3 and CH_4 in the solid/gas molar ratio of 3:13 corresponding to a stoichiometric ratio have been performed at 870, 975, and 1027°C, and the calculated results are shown in Table 1. The first two selected temperatures correspond to the temperature range used in the experiments in this work, while the higher temperature represents a typical temperature used currently for chromium carbide formation by reducing Cr_2O_3. As can be seen, in the product, hydrogen is the main component in the gaseous phase, concentration of methane in the gaseous phase is decreased, and the mole percent of carbon monoxide increases with increasing temperature. On the other hand, the chromium carbide Cr_3C_2 begins to appear in the solid phase only in small concentration at the lower temperature of 870°C. The equilibrium concentration of Cr_3C_2 is rapidly increased with increasing temperature. According to equilibrium calculations, carbon deposition decreases rapidly with increasing temperature directly as a result of the greater stability of the carbide. In practice, C deposition is frequently observed with gaseous reductants, such as methane or carbon monoxide, and must be avoided.

Experimental Procedures

The thermogravimetric method was used to determine the kinetic parameters of the reaction. The experimental setup is shown in Figure 1. In these experiments, the pellets were made using chromium oxide powder, and the pellets were placed inside a platinum basket suspended from a string of an balance with an accuracy of 1 mg. The reactor is a ceramic tube with an inner diameter of 38.7 mm, which is placed in the hot zone of a cylindrical furnace. Initially a stream of argon is allowed to flow through the reactor and, after steady state temperature is achieved (with a heating rate of 5°C/min), it was replaced with a stream of gas mixture, containing methane and argon (at a flow rate of 280 cm^3/min) and the reaction was allowed to proceed. The mole fraction of methane in the input gas mixture was varied between 0.3 and 0.7. The gaseous products that leave from the top of the system are discharged by a suction discharge tube.

The chromium oxide (Cr_2O_3) powder was procured from Merck with a mean particle size of 1 μm and a purity of 99.6%. Figure 2 shows the Scanning Electron Microscopy (SEM) images of the precursor powder of chromium oxide. As can be seen, the particles have no specific geometrical shapes but are distributed as small tubular crystallites or as grains with large aspect ratios. For modeling work in this paper, the average radius of the particle at 0.5 μm is taken as the initial size. Chromium oxide pellets (diameter: 10 mm, thickness: 0.7-5.36 mm, and porosity of 50%±5) were made by mechanical pressing of the powder in a pressing mold. The reduction experi-

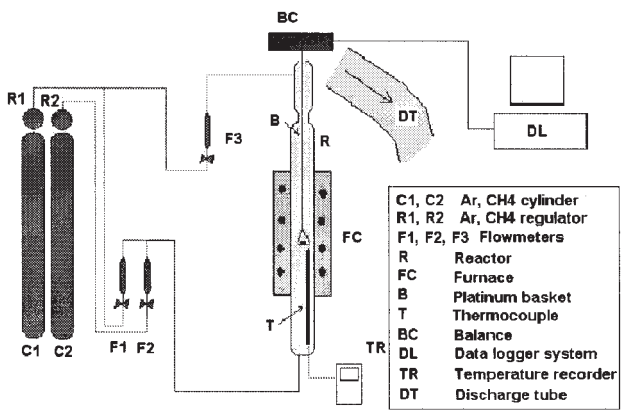

Figure 1. Thermogravimeter setup.

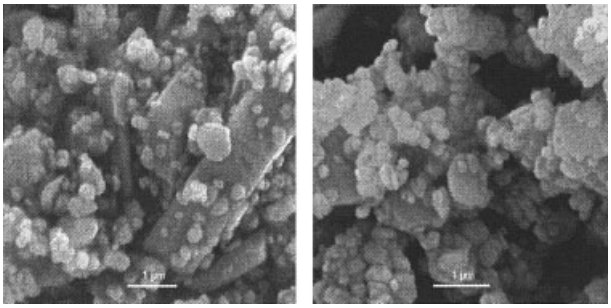

Figure 2. SEM images of chromium oxide.

ments were carried out in the temperature range of 870-975°C under atmospheric pressure.

Experiments were carried out under the condition that the reaction rate is not affected by the gas flow rate. So the external mass transfer resistance was neglected during the reaction.

Two series of experiments were done in the present work. In the first series of experiments, pellets with small thickness were used such that the chemical kinetics controls the overall rate of reaction. In a second series of experiments, pore diffusion was studied, and the experiments were carried out on pellets with relatively large thickness such that diffusion is the controlling step. In these experiments, the pore diffusion was the controlling step of the reaction rate and the pellets were covered in a ceramic shell to control the interface areas contacting the reducing gas. A disk shaped pellet was used, as shown in Figure 3. Using the ceramic shell ensures that the flat shape is maintained, which can be taken as given in the mathematical modeling of the process that will presented in the Discussion section.

Results

The chemical reaction under consideration is expressed by Eq. 1. A typical transient pellet weight vs. time in the TGA during the reaction is shown in Figure 4 at a selected temperature of 925°C and at a selected methane concentration of 0.5 mole fraction. Under the flowing gas open system, while it is assumed that the thermodynamic equilibrium prevails at the reaction site, the continuous supply of fresh reactant accompanied by the continuous removal of the gaseous product sustains the reaction. Therefore, the degree of conversion to the carbide phase is much higher even at a lower temperature in the open

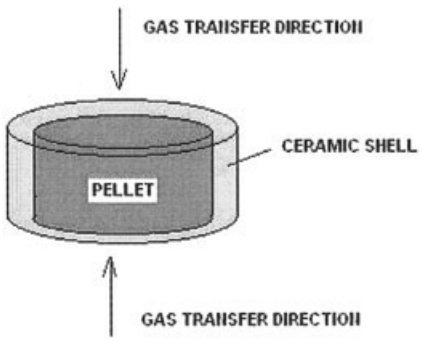

Figure 3. A schematic of shape of pellets used in pore diffusion studies.

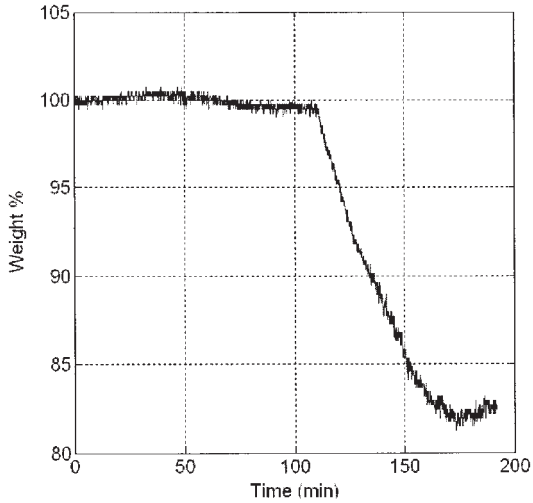

Figure 4. Isothermal reduction curve at T = 925°C and CH_4% = 50.

system than shown in Table 1, which strictly corresponds to a closed system.

Figure 5 shows the XRD pattern of the solid product formed by the reaction, which corresponds to the phase Cr_3C_2 that in this case was produced at a temperature as low as 870°C. Often graphite phase formation can be seen visually, but under these conditions, there was no evidence for graphite deposition. The graphite carbon deposition is not seen in the XRD pattern or in electron microscopy on samples reduced even at a temperature as low as 870°C. Lack of any evidence for the formation of graphite is applicable to the current experimental situation, but the result is seen as favorable for providing the rationale for further developing a process based on the current findings. Both the presence of water vapor and the formation of carbon dioxide in the gas phase are known to prevent or minimize carbon deposition.[5-7] This can be further helped by any catalytic activity for carbon gasification of the carbide product. Further work will be carried out to ascertain the exact reasons for the prevention of carbon deposition.

Under the above conditions, it is reasonable to assume that weight change of the chromium oxide pellets is based on conversion to the chromium carbide Cr_3C_2. without any carbon deposition. The "conversion" is defined as the weight of a pellet at a given time divided by the pellet weight when it is

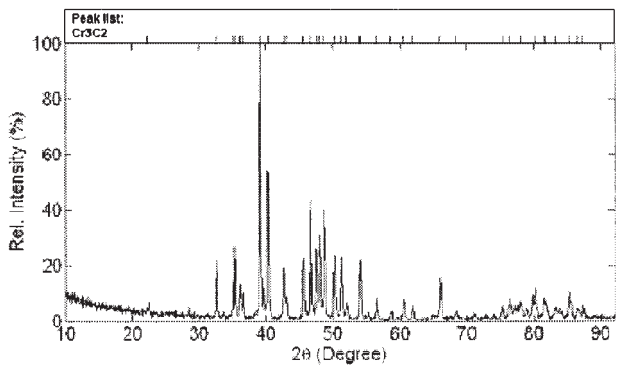

Figure 5. XRD pattern of Cr_3C_2 produced at T = 870°C.

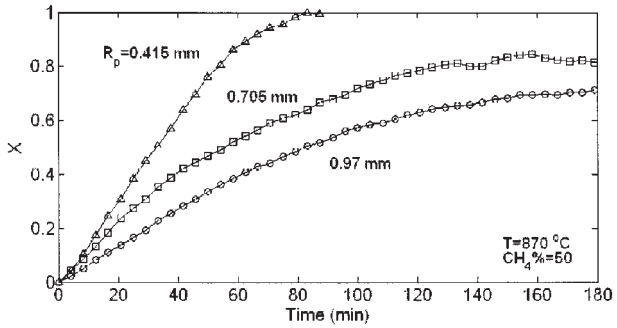

Figure 6. Isothermal reduction curves at T = 870°C for pellets with different thicknesses.

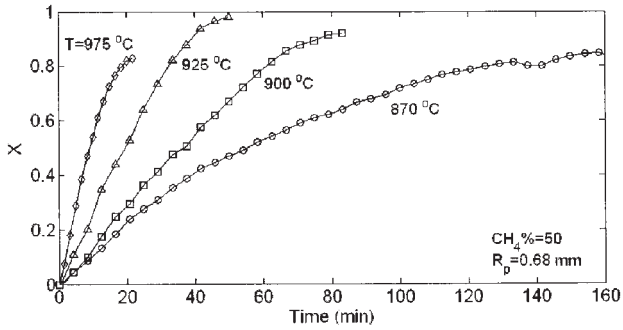

Figure 8. Isothermal reduction curves at different temperatures and $CH_4\%$ = 50.

completely reduced, i.e., all the oxygen atoms are liberated from it. Thus, the conversion-time curves can be obtained from the weight change curves using the following relation that was derived from stoichiometry of the reaction [1]:

$$X(t) = \frac{151.99\left(100 - \frac{W(t)}{W_0}\%\right)}{300\left(16 - \frac{16}{3}\right)} \tag{3}$$

where W(t) and W_0 are the transient and initial pellet weights, respectively.

The isothermal reduction curves of X vs. time are shown in Figure 6 for pellets with thicknesses of 0.83 mm, 1.41 mm, and 1.94 mm (R_P is defined as a half thickness of the pellet) and at methane mole fraction of 0.5. As can be expected, the time needed to obtain a specified value of conversion is lower for pellets with a smaller thickness. Figure 7 shows isothermal reduction curves at a fixed temperature of 925°C for pellets with an average thickness of 1.4 mm (±0.02 mm) with varying methane mole fractions of 0.3 and 0.5. As is expected, the gas streams containing higher mole fraction of methane can reduce the pellets in lesser time.

Isothermal reduction curves are shown in Figure 8 for samples at different temperatures between 870-975°C using pellets with an average thickness of 1.36 mm (±0.02 mm) and a fixed concentration of methane at a mole fraction of 0.5. This Figure shows the effect of temperature on reduction curves for constant pellet geometry and a constant reducing condition in the gas mixture. The reaction rate is clearly accelerated by increasing the temperature. As mentioned in the previous section regarding a number of experiments that were carried out on the pellets with relatively large thickness (4.19 mm and 5.36 mm), where pore diffusion is the limiting factor, the kinetic data can be used to study the pore diffusion effect on the reaction rate. Thus, the kinetic data can be used to study the pore diffusion effect on the reaction rate. Figure 9 shows the weight change curve for a pellet with a thickness of 4.19 mm reduced at a temperature of 940°C with methane concentration at a mole fraction of 0.5. The isothermal reduction curves calculated from Figure 9, using Eq. 3, are shown in Figure 10 for pellets with a thickness of 4.19 mm at a temperature of 940°C and for pellets with a thickness of 5.36 mm at different temperatures of 935 and 951°C (R_P is defined as a half thickness of the pellet). The combined effects of temperature and pellets are evident in the data.

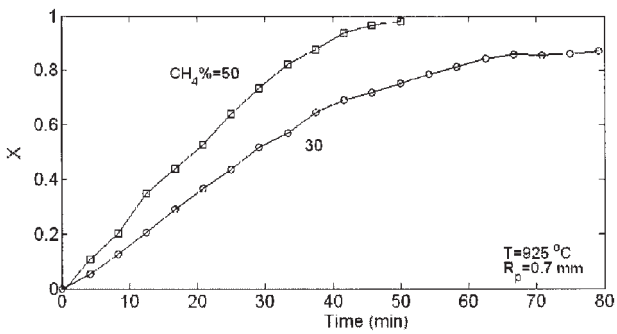

Figure 7. Isothermal reduction curves at T = 925°C for different methane mole fractions.

Discussion

Reaction rate controlled reduction

In the first part of the experiments (Figures 6-8), the chemical kinetics controls the overall rate of reaction and indeed

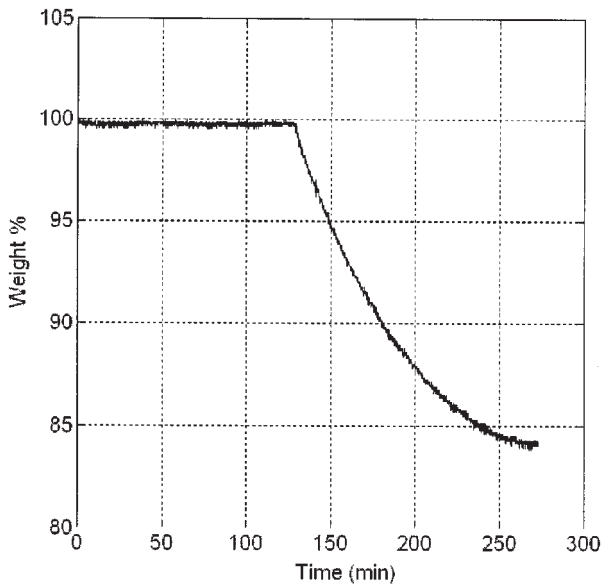

Figure 9. Weight change curve at T = 940°C for pellet with R_P = 2.095 mm.

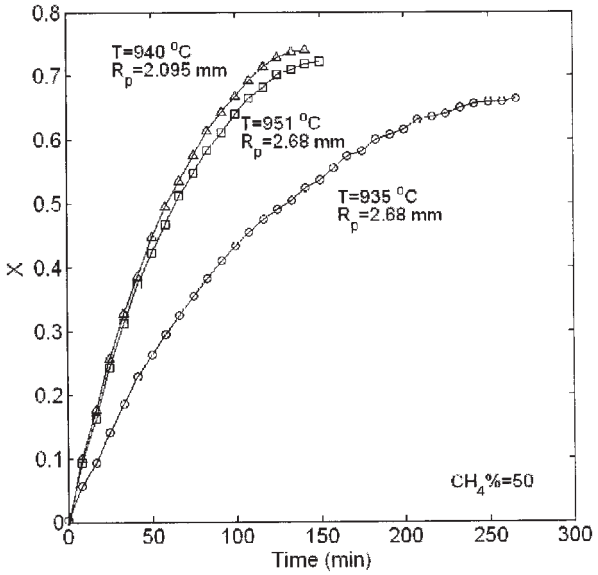

Figure 10. Isothermal reduction curve at different temperatures for pellets with different thicknesses.

external mass transfer effect and the pore diffusion effect were neglected because of using sufficiently high gas flow rate (280 cm^3/min) and pellets with relatively small thicknesses. The grain model, as described in detail by Szekely et al.,[8-10] was used to calculate the kinetic parameters. Using this model, reduction of chromium, manganese, and cobalt oxides with methane were described in detail by Khoshandam[11] and Khoshandam et al.[12]

To specify the grain shape factor, F_g, the method proposed by Szekely et al.[8] was used in this work. The method consists of plotting $1 - (1 - X)^{1/Fg}$ vs. time at different values of F_g (1, 2, and 3 for flat plate, cylindrical, and spherical shape grains, respectively) and then selecting F_g from the best form of linearity through the curves. The grain shape factor could be in many cases an empirical model parameter, although when the pellets are produced by compaction, it could have a physical basis. The plot of $1 - (1 - X)^{1/Fg}$ vs. time is shown in Figure 11 for a typical pellet with a thickness of 0.72 mm at a reduction temperature of 900°C and the gaseous concentration of methane at a mole fraction of 0.5. As is seen, the best value for linearity corresponds to F_g of 2, implying a cylindrical shape for grains. Given the high aspect ratio of some of the grains and the crystalline nature of the tubular grains as shown in Figure 2, the best-fit lines reflect the physical situation quite well.

As observed in Figure 7, the slope of X vs. time (dX/dt) increases from about 0.018 min^{-1} to 0.031 min^{-1} (about 1.7 times) with increasing methane concentration from 0.3 to 0.5 mole fraction. At the methane mole fraction of 0.5, the reaction can also be described as a first order reaction with respect to methane concentration.

For a generalized reaction A(g) + bB(s) = cC(g) + dD(s), the ratio of molar volume of solid product to solid reactant, Z_v, is defined as follows:

$$Z_v = \frac{d\rho_B M_D}{b\rho_D(1-\varepsilon_D)M_B} \tag{4}$$

where d and b are stoichiometric coefficients of solid product D and solid reactant B, respectively, ρ is density, M is molecular weight, and ε_D is porosity of solid product D. Actually, the structural changes of pellets during the course of the reaction can be calculated from knowing Z_v. If the value of Z_v is smaller, equal, and larger than 1, the pellet dimensions would be smaller than initial state, no change, and larger than initial state, respectively. In the present reaction, Z_v was calculated between 0.6 and 1.2, so the structural changes of pellets can be neglected during the course of the reaction.[8]

By ignoring structural change of the pellets, the generalized modulus of gas-solid reaction $\hat{\sigma}$, is defined as follows for flat pellets that are made from cylindrical grains[8]:

$$\hat{\sigma} = R_P\sqrt{\frac{(1-\varepsilon)k}{2D_e r_g}} \tag{5}$$

where R_P is a half thickness of the pellet, ε is the pellet porosity, k is the reaction rate constant, D_e is effective diffusion coefficient of gaseous reactant in the pellet, and r_g is the radius of grains.

The following relationship is given for small values of $\hat{\sigma}$ (<0.3) for cylindrical grains based on the grain model[8-10]:

$$1-(1-X)^{1/2} = (1-C_1HR_P^2)\frac{bkC_{CH_4,b}}{r_g\rho_{Cr_2O_3}}t \tag{6}$$

where C_1 and H are constants and $C_{CH_4,b}$ is methane molar concentration in the gas stream.

Plotting $1 - (1 - X)^{1/2}$ vs. time results, the slope can be shown to be:

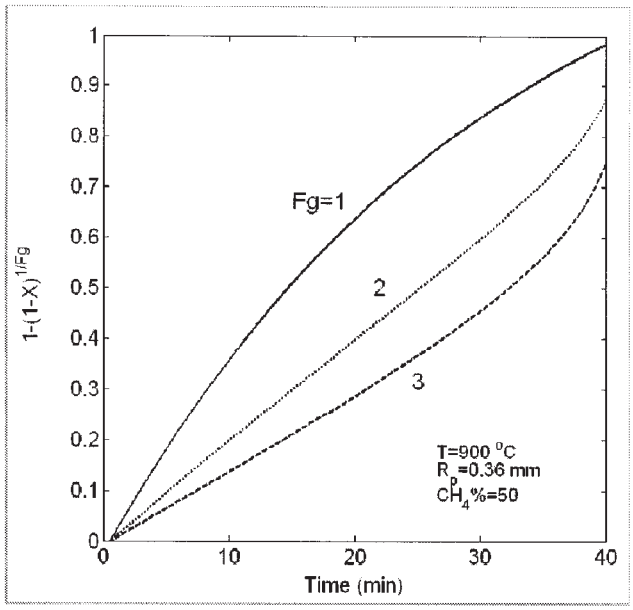

Figure 11. $1 - (1 - X)^{1/Fg}$ vs. time at T = 900°C.

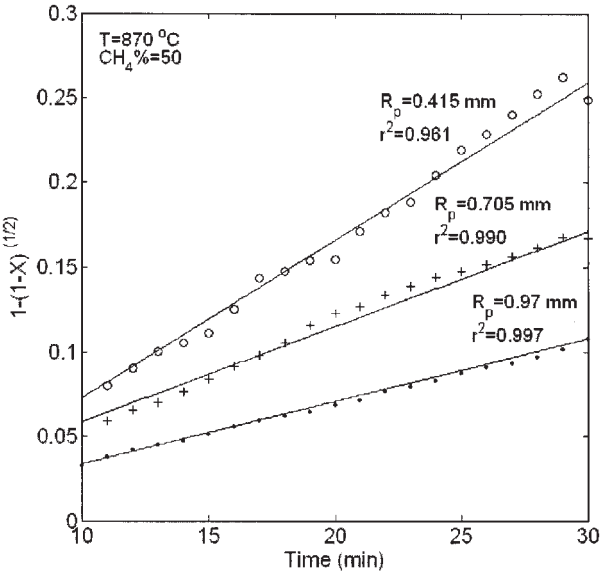

Figure 12. $1 - (1 - X)^{1/2}$ vs. time at T = 870°C, CH_4% = 50, and for different thicknesses.

$$slope = \frac{bkC_{CH_4,b}}{r_g\rho_{Cr_2O_3}} - \frac{C_1HkbC_{CH_4,b}}{r_g\rho_{Cr_2O_3}}R_P^2 \tag{7}$$

A plot of $1 - (1 - X)^{1/2}$ vs. time is shown in Figure 12 for pellets with different thicknesses at temperature of 870°C and a methane mole fraction of 0.5. As is seen, the slopes increase with decreasing pellet thickness.

The reaction rate constant k can be calculated from the intersection at the y-axis of the plot of the slope vs. R_P^2 plotted at a constant temperature and a constant concentration of methane based on Eq. 7. The plot of slope vs. R_P^2 is shown in Figure 13 for pellets that were reduced at temperature of 870°C at a concentration of methane at a mole fraction of 0.5. The

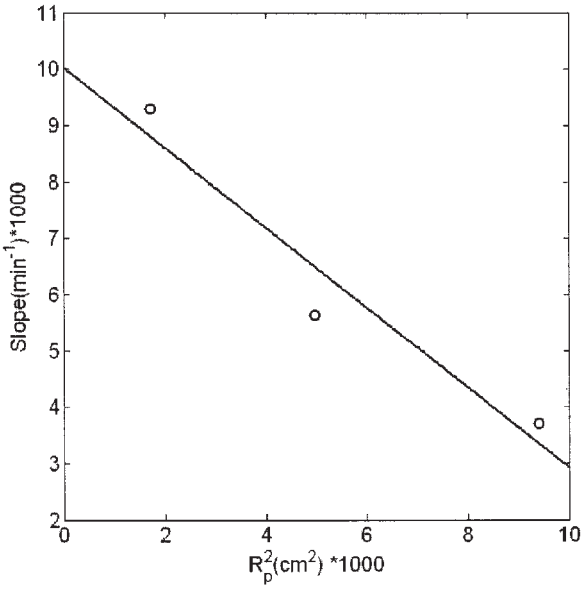

Figure 13. Slope vs. R_P^2 at T = 870°C and CH_4% = 50.

Table 2. The Reaction Rate Constants at Different Temperatures

Temperature (°C)	870	900	925	950	975
k (mm/sec)	0.0025	0.0048	0.0074	0.0082	0.0165

reaction rate constant is calculated as follows from the intersection of 0.01 at temperature of 870°C:

$$k\ (\text{mm/sec}) = (0.01)\frac{(1000)}{60}\frac{r_g\rho_{Cr_2O_3}}{bC_{CH_4,b}} \tag{8}$$

In this equation, the grain radius, r_g, can be estimated from:

$$r_g = \left(\frac{d}{b}\frac{r_0^{F_g}}{(1-\varepsilon_D)}\frac{\rho_B M_D}{\rho_D M_B}\right)^{1/F_g} \tag{9}$$

where r_0 is the initial grain radius (0.5 μm) taken from the particle size measurement described in the Experimental Procedures section. The reaction rate constants can be calculated using similar procedures for different temperatures. The numerical values of the reaction rate constants at different temperatures are given in Table 2. The Arrhenius plot is shown in Figure 14 and, based on the figure, the activation energy of the reaction is calculated from the slope as 193.5 kJ/mol.

Pore diffusion controlled reduction reaction

As mentioned before, a number of experiments were carried out on pellets with large thickness. In this situation, the pore diffusion controls the overall rate of reaction because of the long diffusion path through the pellet. Using these experiments, the effective diffusion coefficient is calculated through the porous pellets.

For large values of $\hat{\sigma}$ (>2.0), the relationship between the

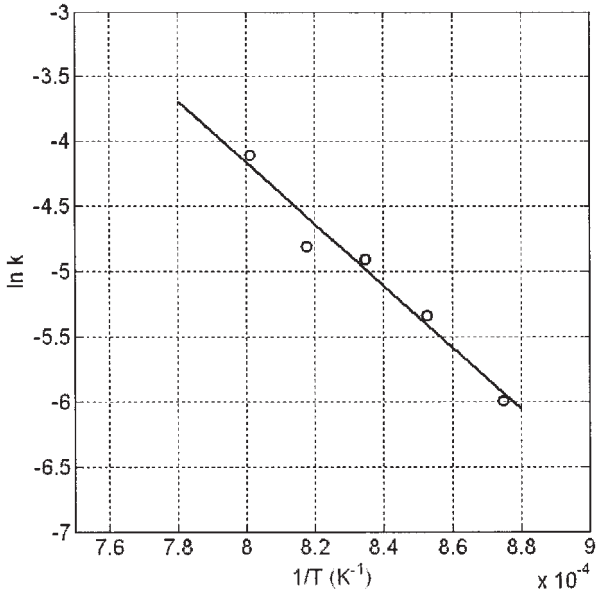

Figure 14. Arrhenius curve, $Lnk = -2.37 \times 10^4(1/T) + 14.8$, k in mm/s.

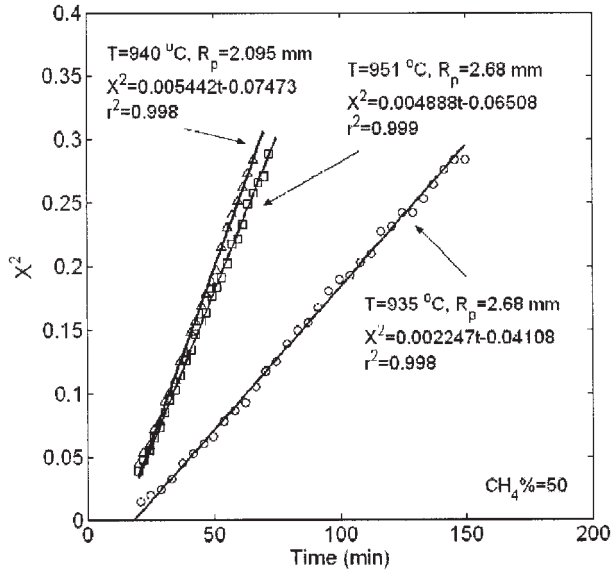

Figure 15. X^2 vs. time at temperatures of 935, 940, and 951°C and $CH_4\%$ = 50 for pellets with different thicknesses.

(The symbols show the experimental data.)

conversion X and time t is written as follows for the flat shape pellets based on the grain model[8]:

$$X^2 = \frac{2bD_eC_{CH_4,b}}{R_P^2(1-\varepsilon)\rho_{Cr_2O_3}}t - \frac{1}{2\hat{\sigma}^2} \tag{10}$$

In this equation the initial porosity of the pellet, ε, can be estimated using calculation of the pellet volume from pellet geometry and measuring the weight of the pellet.

The effective diffusion coefficient D_e is calculated from the slope of X^2 vs. time. Figure 15 depicts the plot of X^2 vs. time for pellets with different thickness at temperatures of 935, 940, and 951°C. The calculated D_e values are given in Table 3.

The pore diffusion controls the overall rate of reaction—considering the bulk flow effect

The bulk flow effect can be significant in reduction reactions using methane as a reducing agent because of volume change between gaseous products and gaseous reactants, as expressed in Eq. 1. Considering bulk flow effect, the methane molar flux inside the pellets can be expressed as follows:

$$N_{CH_4} = y_{CH_4}\sum_{i=1}^{n_c} N_i - D_e\frac{\partial C_{CH_4}}{\partial z} \tag{11}$$

Table 3. Calculated Values of D_e

Run	T (°C)	R_P (mm)	ε (%)	$C_{CH_4,b}$ (kmol/m^3)	D_e (cm^2/sec)	$\hat{\sigma}$
1	935	2.68	44.52	0.005	0.0221	3.6
2	940	2.095	49.58	0.005	0.0299	2.3
3	951	2.68	49.70	0.005	0.0438	2.6

Table 4. Calculated Values of D_e

Run	T (°C)	R_P (mm)	ε (%)	$y_{CH_4,b}$	D_e (cm^2/sec)	$\hat{\sigma}$
1	935	2.68	44.52	0.5	0.03061	4.4
2	940	2.095	49.58	0.5	0.04117	3.1
3	951	2.68	49.70	0.5	0.06037	3.5

where N is molar flux, y is mole fraction, n_c is number of components in the gas phase, and $\partial C_{CH_4}/\partial z$ is concentration gradient of methane in the pellet.

The effective diffusion coefficient of gas through the pellet is calculated from the following relation for flat pellets[13]:

$$X^2 = \frac{2bC_tD_eLn[1+y_{CH_4,b}(c-1)]}{R_P^2(1-\varepsilon)\rho_{Cr_2O_3}(c-1)}t \tag{12}$$

where C_t is total molar concentration of the gas mixture, $y_{CH_4,b}$ is methane mole fraction in methane-argon mixture, and c is stoichiometric coefficient of the gas product.

The effective diffusion coefficient D_e can be calculated from the slope of X^2 vs. time. The plot of X^2 vs. time is shown in Figure 15 for pellets with different thicknesses at different temperatures of 935, 940, and 951°C. The values calculated for D_e are given in Table 4.

The comparison between the values obtained for D_e in two cases, with and without considering bulk flow effect, is given in Table 5. As is seen, the error of 27% appeared in calculated D_e when we ignore the bulk flow effect.

Estimation of diffusion coefficient of gas through the product layer around the grains

The experiments carried out for kinetic parameters determination can be used to estimate the diffusion coefficient of gas through the product layer around the grains. The relation between conversion and time is as follows for cylindrical grains considering the bulk flow effect and diffusion through the product layer around the grains:

$$t = \frac{1-(1-X)^{1/2}}{\dfrac{bkC_{CH_4,b}}{\rho_{Cr_2O_3}r_g}} + \frac{\rho_{Cr_2O_3}r_g^2}{4D_{CH_4,P}bC_{CH_4,b}}\frac{\theta}{Ln(1+\theta)} \times [X+(1-X)Ln(1-X)] \tag{13}$$

where $D_{CH_4,P}$ is the diffusion coefficient of methane through the product layer around the grains and θ is defined as follows:

$$\theta = y_{CH_4,b}(c-1) \tag{14}$$

Table 5. A Comparison Between Values Calculated for D_e

Run	D_e (cm^2/sec)[a]	D_e (cm^2/sec)[b]	Error (%)
1	0.0221	0.03061	27.8
2	0.0229	0.04117	27.4
3	0.0438	0.06037	27.5

[a]Without considering bulk flow effect.
[b]Considering bulk flow effect.

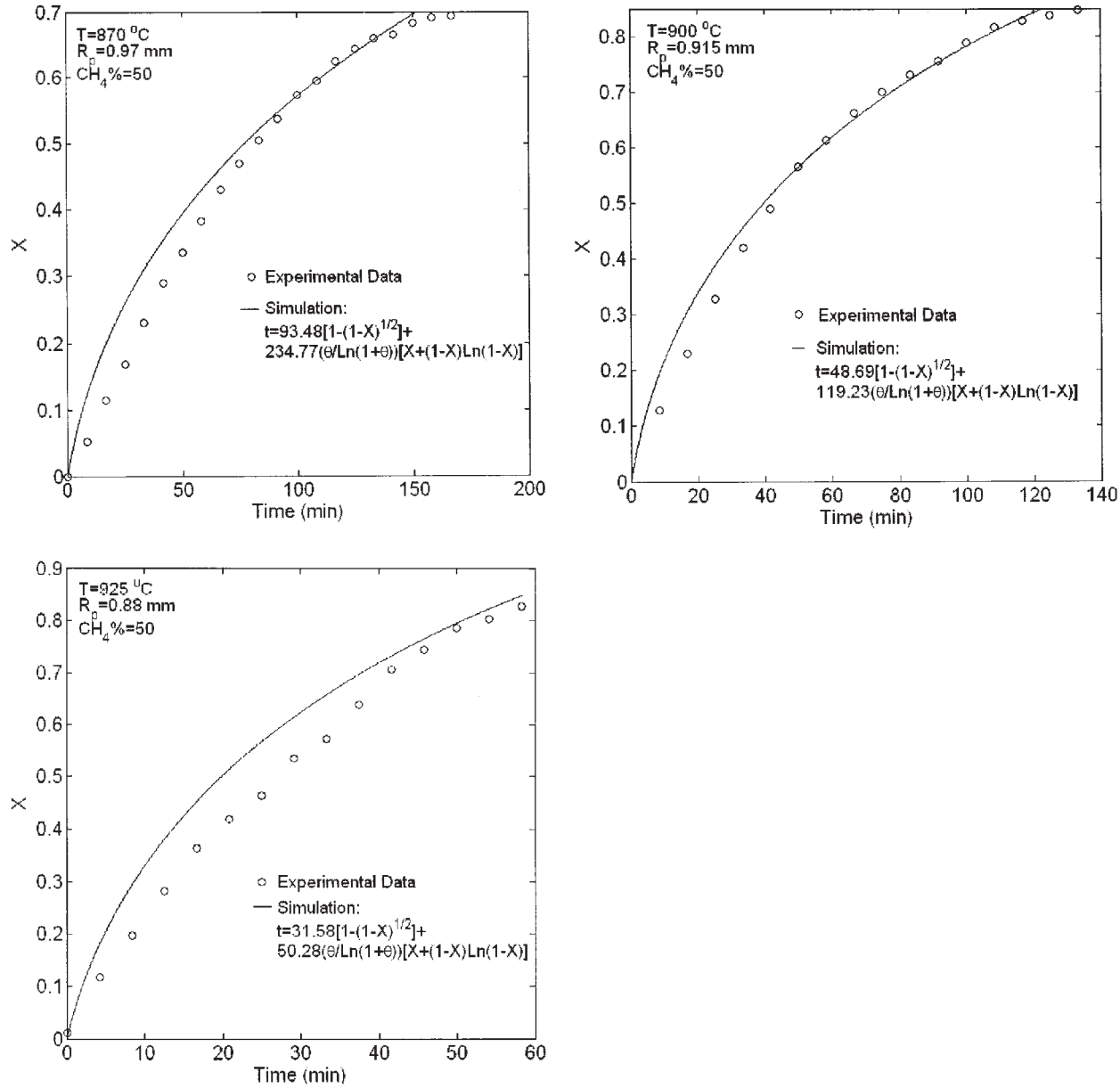

Figure 16. X vs. time at different temperatures and CH_4% = 50 for pellets with different thicknesses.

(The symbols show the experimental data, and the solid lines show the best fit based on Eq. 13.) (a) Thickness of 1.94 mm at T = 870°C, (b) Thickness of 1.83 mm at T = 900°C, (c) Thickness of 1.76 mm at T = 925°C.

All the parameters on the right hand side of Eq. 13 are known except for $D_{CH_4,P}$ in a given experiment. The best value for $D_{CH_4,P}$ can be obtained using the best fit of Eq. 13 with the experimental data. The curve fitting toolbox 1.1 in MATLAB ver. 6.5 was used for data fitting. The best fitting of the data on Eq. 13 is shown in Figure 16 under the different operating conditions. The values calculated for $D_{CH_4,P}$ are given in Table 6 and, as expected, these values increase with temperature.

Conclusions

In the present work, chemical reaction between methane and chromium oxide was studied. Solid chromium carbide (Cr_3C_2) was formed as the reaction product, and it could be produced at a temperature as low as 870°C, at least 140°C below the temperature quoted for other conventional methods with carbon (or CO formed in situ) as the reducing agent. The kinetic parameters of the reaction were calculated at temperature range of 870-975°C and under atmospheric pressure combining experimental results from thermogravimetric analysis with a mathematical model based on the grain model developed by Szekely et al.[8]

Table 6. Calculated Values of D_{AP}

Run	T (°C)	R_P (mm)	$y_{CH_4,b}$	k (mm/sec)	$D_{CH_4,P} \times 10^9$ (cm^2/sec)
1	870	0.97	0.5	0.0025	1.24
2	900	0.915	0.5	0.0048	2.45
3	925	0.88	0.5	0.0074	5.81

Notation

b, d = stoichiometric coefficients of solid reactant and solid product, respectively
c = stoichiometric coefficient of the reaction gas product
C_1 = a constant in Eq. 6
$C_{CH_4,b}$ = methane molar concentration in the gas stream
C_t, C = total molar concentration and molar concentration of the gas stream, respectively
$D_{CH_4,P}$ = diffusion coefficient of methane in the product layer around the grains
D_e = effective diffusion coefficient of methane in pellet
H = a constant in Eq. 6
k = reaction rate constant
K_P = equilibrium constant of reaction based on the partial pressures
M = molecular weight
n_c = number of components in the gas mixture
N = molar flux
r_g, r_0 = grain radius and initial grain radius, respectively
R_P = half thickness of the pellet
T = temperature
t = time
$W(t)$, W_o = transition and initial weight of the pellet, respectively
X = conversion
$y_{CH_4,b}$ = methane mole fraction in the bulk of gas
z = gas diffusion direction through the pellet
Z_v = ratio of molar volume of solid product to solid reactant
ε = porosity of pellet
θ = a parameter defined in Eq. 14
ρ = density
$\hat{\sigma}$ = generalized modulus of gas-solid reaction defined in Eq. 5

Subscripts

B, D = solid reactant and product, respectively
CH_4 = methane
Cr_2O_3 = chromium oxide
i = gaseous component

Literature Cited

1. Samsonov GV. *Refractory Carbides*. New York: Consultants Bureau. 1974.
2. Popov AA, Ostrik PN, Gasik MM. Thermodynamics of reduction and carbide formation in the Cr-C-O system. *Izv Vyssh Uchebn Zaved Chern Metall.* 1986;29(10):1-3.
3. Berger LM, Stolle S, Gruner W, Wetzig K. Investigation of the carbothermal reduction process of chromium oxide by micro- and lab-scale methods. *International Journal of Refractory Metals & Hard Materials.* 2001;19:109-121.
4. http://gttserv.lth.rwth-aachen.de/~cg/Software/FactSage/IndexFrame.htm.
5. Khoshandam B, Kumar RV, Jamshidi E. Simulation of non-catalytic gas-solid reactions: application of grain model for the reduction of cobalt oxide with methane. *Mineral Processing & Extractive Metallurgy (Trans. IMM C).* 2005;114:10-22.
6. Ramachandran PA, Doraiswamy LK. Modelling of non-catalytic gas-solid reactions. *AIChE Journal.* 1982;28:881-900.
7. Stobbe ER, de Boer BA, Geus JW. The reduction and oxidation behaviour of manganese oxides. *Catalysis Today.* 1999;47:161-167.
8. Szekely J, Evans JW, Sohn HY. *Gas Solid Reactions*. New York: Academic Press Inc.; 1976.
9. Szekely J, Lin CI, Sohn HY. A structural model for gas-solid reactions with a moving boundary—V: An experimental study of the reduction of porous nickel-oxide pellets with hydrogen. *Chemical Engineering Science.* 1973;28:1975-1989.
10. Szekely J, Sohn HY. Effect of structure on the reaction between a porous solid and a gas. *Transactions of the Institution of Mining and Metallurgy—Section C.* 1973;82:C92-C100.
11. Khoshandam B. Reduction of chromium, manganese and cobalt oxides with methane. Ph.D. thesis, Amir-Kabir University (Tehran Polytechnic), 2004.
12. Khoshandam B, Kumar RV, Jamshidi E. Reduction of cobalt oxide with methane, *Metallurgical and Materials Transactions B*. 2004;35B: 825-828.
13. Sohn HY, Bascur OA. Effect of bulk flow due to volume change in the gas phase on gas-solid reactions: initially porous solids. *Industrial and Engineering Chemistry: Process Design and Development.* 1982;21: 658-663.

Manuscript received Apr. 13, 2005, and revision received Sept. 8, 2005.